ISSN 0018-1439, High Energy Chemistry, 2019, Vol. 53, No. 3, pp. 246–253. © Pleiades Publishing, Ltd., 2019.
Russian Text © The Author(s), 2019, published in Khimiya Vysokikh Energii, 2019, Vol. 53, No. 3, pp. 235–242.

PLASMA CHEMISTRY

Reduction of Boron Trichloride in Atmospheric-Pressure Argon–Hydrogen Radiofrequency Induction Plasma

R. A. Kornev[a], *, P. G. Sennikov[a], L. V. Shabarova[a], A. I. Shishkin[b], T. A. Drozdova[b], and S. V. Sintsov[c]

[a] *Devyatykh Institute of Chemistry of High-Purity Substances, Russian Academy of Sciences, Nizhny Novgorod, 603951 Russia*

[b] *Nizhny Novgorod State Technical University, Nizhny Novgorod, 603115 Russia*

[c] *Institute of Applied Physics, Russian Academy of Sciences, Nizhny Novgorod, 603950 Russia*

**e-mail: kornev@ihps.nnov.ru*

Received November 6, 2018; revised December 26, 2018; accepted December 28, 2018

Abstract—The main operating modes of a radiofrequency induction plasma torch with a vortex stabilization of the atmospheric-pressure gas discharge at have been studied in an argon-hydrogen mixture in the range of $Ar/H_2 = 12–4$. The dependences of the electron temperature T_e and number density n_e on the Ar/H_2 ratio have been experimentally studied. It has been found that the electron temperature and concentration in pure argon plasma are 0.88 eV and 7.6×10^{14} cm^{-3}, respectively. When the Ar/H_2 ratio decreases, the electron temperature decreases to 0.42 eV, and the electron number density is 8×10^{12} cm^{-3}. The calorimetric method used to estimate the gas temperature T_g, has given a value of 2500 K. The process of BCl_3 reduction with hydrogen has been studied at the implemented operating modes of the induction plasma torch. The main products of the reduction of boron trichloride are a polycrystalline boron powder and dichloroborane. The morphology of boron and its phase composition and impurities have been studied. The average particle size of the boron powder is 200 nm.

Keywords: radiofrequency induction plasma torch, emission spectroscopy, boron trichloride, nanoboron

DOI: 10.1134/S001814391903010X

INTRODUCTIoN

The development of plasma-chemical processes based on radiofrequency induction (RFI) plasma torches is an urgent task, since the use of plasma torches allows high-enthalpy processes to be carried out and ensures chemical purity of the high-temperature region created by plasma, and high productivity [1–5]. In the development of plasma-chemical processes using an RFI plasma torch, it is necessary to determine the main plasma parameters: gas temperature T_g and electron number density n_e which, in turn, are affected by main technological parameters, in particular, the reactant ratio and energy input. Experimental data on the temperature and number concentration of electrons, as well as the gas temperature, under the conditions of an atmospheric-pressure inductively coupled RF discharge can be obtained using optical emission spectroscopy [6–10].

The process of hydrogen reduction of BCl_3 in equilibrium plasma has been studied. For example, the yield of elemental boron in an arc discharge was found to be 70% using a plasma device a 8–20 kW power with the plasma-forming gas 80% H_2 + 20% Ar at flow rate of 100 L/min and an H_2/BCl_3 ratio of ≥ 5. The boron samples obtained were heavily contaminated with impurities from the electrode material, and the efficiency of the process for the desired product did not exceed 10% [11]. Cueilleron and Cruiziat [12] achieved approximately the same yield in an argon–hydrogen jet using an RF apparatus at high flow rate (up to 16 L/min) of plasma gas (10% H_2 + 90% Ar), a chloride vapor flow rate of 0.11–0.22 L/min, and a plasma temperature of 10.000 K. Murdoch and Hamblyn [13] patented a process in which the yield of elemental boron could be as high as 30% with the use of an RFI plasma torch at an optimal plasma-forming gas (75% H_2 + 25% Ar) flow rate of 40 L/min and an H_2/BCl_3 molar ratio of 2.6. It was reported that a fine-crystalline powder with a particle size of 1.7 μm is produced under these conditions. The boron concentration in the product sample was as high as 99%. It should be noted that modern composite materials with high mechanical strength based on boron and its carbide require a powder material with a particle size of 50–300 nm and an impurity content of 10^{-3} at % [14]. Neither this purity level nor the required particle size was achieved in the studies cited.

The purpose of this work is to experimentally determine the main parameters of argon–hydrogen plasma (electron temperature and number density) in a gas-vortex stabilized RFI plasma torch at various Ar/H_2 ratios, study the hydrogen reduction of BCl_3,

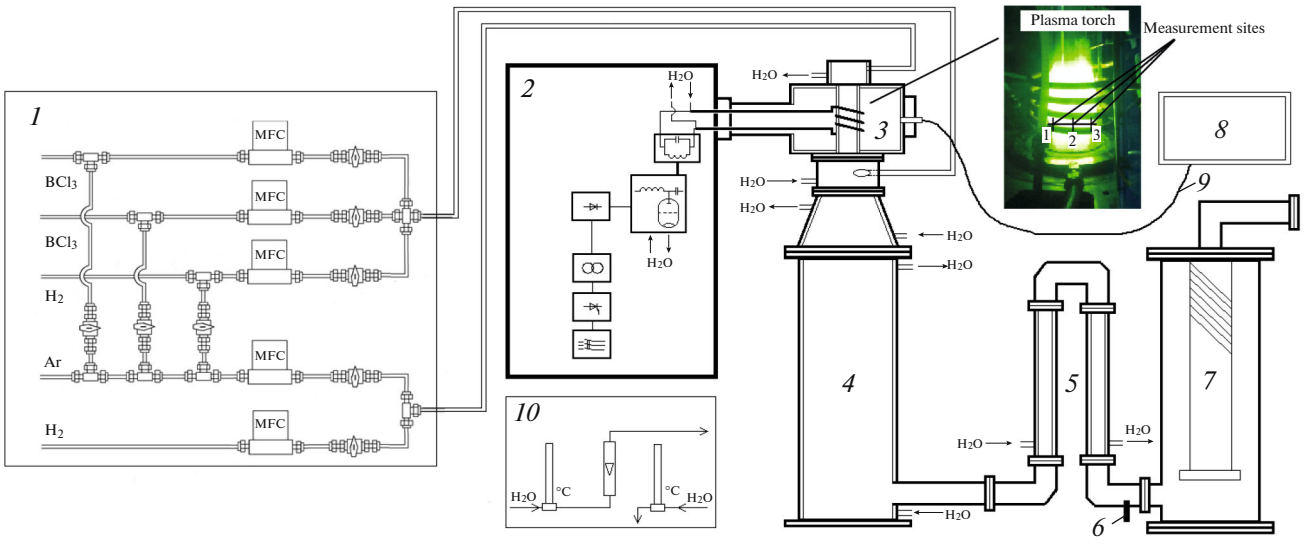

Fig. 1. Schematic diagram of the RF setup with the RFI plasma torch: (*1*) gas panel, (*2*) RF generator ($f = 5.28$ MHz), (*3*) RFI plasma torch, (*4*) plasma reactor, (*5*) condenser, (*6*) thermocouple, (*7*) filter, (*8*) emission spectrometer, (*9*) optical fiber, (*10*) calorimeter.

and obtain samples of finely divided high-purity boron.

EXPERIMENTAL

Our experimental study of the RFI plasma torch was carried out using the setup schematically shown in Fig. 1. The RF generator frequency was 5.28 MHz. The RFI plasma torch was a quartz tube around which an induction coil was wound. In the upper part of the quartz tube, a head with a swirler was placed to provide tangential feed of the plasma gas to the discharge zone.

The RFI plasma torch was started-up at atmospheric pressure using a Tesla coil spark ignition device. Both pure argon and a mixture of argon with hydrogen were used as a plasma gas. To evaluate the power absorbed by the gas discharge, the following heat balance equation was used:

$$W_{in} = W_d + W_l, \quad (1)$$

where W_{in} is the power supplied to the plasma torch from the generator; W_d is the power absorbed by the gas discharge; and W_l is the power released in the generator–plasma torch elements.

The value of W_{in} was measured using an automated generator control system, and the value of W_l was measured using a water calorimeter. Thus, W_d was determined to be 25 kW. The volume velocity of the plasma gas Ar + H_2 was 100 L/min in this case. The specific energy input P (kJ/mol) was calculated based on the values of power W_p (W) and plasma gas mass flow rate Q (mol/s) according to the equation:

$$P = W_p/Q \quad (2)$$

and was kept constant at 350 ± 25 kJ/mol. The power absorbed by the gas discharge is spent for gas heating (W_g) and radiation (W_r):

$$W_d = W_g + W_r. \quad (3)$$

In this experiment, both of these components were measured using a water calorimeter. It was believed that radiation is absorbed completely by a plasma torch shield. Therefore, for measuring W_r, water cooling of the shield was provided. The power picked up by the calorimeter from the plasma torch shield was 4 kW. For measuring W_g, water cooling was also provided in the plasma reactor and in the condenser specially designed for cooling the exhaust gas. The gas temperature at the plasma torch inlet was assumed to be 25°C, and it was 35 ± 5°C at the outlet from the condenser, as measured with a thermocouple. The power picked up by the calorimeter from the cooling device was 18 kW. Thus, the value of W_d determined according to Eq. (3) was 22 kW, in agreement with the value determined using Eq. (1).

The Ar/H_2 ratio during the experiments varied from 4 to 12. The range is determined by effective operation of the RFI plasma torch. As is known [15], when gaseous substances of a complex composition are added to a monatomic gas, a significant portion of the energy is spent on their vibrational pumping and dissociation, which leads to redistribution of the gas temperature followed by an increase in plasma resistance. In this case, an increase in the electric current in the induction coil is required to maintain the gas discharge. In practice, this requires an increase in the power input. Otherwise, the discharge is extinguished. When $Ar/H_2 < 4$ and the power input in the discharge

is maximal, the gas discharge is extinguished because of a high concentration of the high-enthalpy gas (hydrogen) in the mixture. When the Ar/H_2 ratio is higher than 12 and the minimum power is supplied to the discharge, the gas discharge is extinguished because of the heating and destruction of the quartz flask of the RFI plasma torch. Thus, the molecular gas H_2 added plays the role of a buffer, which takes up some of the energy transferred from plasma free electrons, thereby, on one hand, preventing the overheating of the plasma torch walls and, on the other hand, becoming active, which is important for hydrogen reduction processes.

The gas temperature for the $Ar/H_2 = 6$ mixture at the outlet of the plasma torch was determined using the equation

$$W_g = C_p Q(T_g - T), \quad (4)$$

where C_p is the heat capacity of the gas mixture; Q is the flow rate of the gas mixture; and T_g and T are the gas temperatures at the outlet and inlet of the plasma torch, respectively. The value of T_g is 2500 K.

Plasma emission spectra of pure argon and its mixture with hydrogen were recorded in the range of 300–900 nm using an Ocean Optics HR4000CG-UV-NIR fiber optic spectrometer with a resolution of 0.3 nm and a COL-UV/VIS collimation lens. The emission spectra were recorded at three points along the plasma torch diameter as shown in Fig. 1. Based on the spectroscopic data, we estimated the electron temperature in the plasmas of pure argon and the Ar/H_2 mixture with the reactant ratio varying from 4 to 12.

Plasma under study is considered as a system of particles, the interaction between which determines the main characteristics of the plasma and, in particular, creates a radiation field. It should be noted that each process in plasma can be compared to its reverse process: excitation–de-excitation, ionization–recombination, etc. According to the principle of detailed equilibrium, the rates of forward and reverse processes are equal. Therefore, as a result, the distribution of electrons over energy levels is established to be the same as at full thermodynamic equilibrium. In this case, the number of excited molecules is determined by the Boltzmann law. The parameter of this distribution is the electron temperature, and the proportionality coefficient includes only atomic constants. Therefore, it is possible to determine the electron temperature by measuring the number of excited atoms.

The number of excited atoms can be judged by the number of photons emitted. In practice, the intensity of the spectral band is usually measured, which is proportional to the number of emitted photons. The spectral band intensity means the radiation power of a given frequency emitted by plasma at a certain solid angle determined by the experimental conditions [10]. A unit volume of plasma emits radiation into unit solid angle with an intensity equal to:

$$I_{ki} = \frac{1}{4\pi} n_k A_{ki} h\nu_{ki} = \frac{1}{4\pi} n_0 \frac{g_k}{g_0} A_{ki} h\nu_{ki} \exp\left(-\frac{E_k}{kT_e}\right). \quad (5)$$

Measuring the relative intensities of two emission lines and knowing the atomic transition constants, one can determine the electron temperature by comparing these intensities with each other [16]:

$$\frac{I_{ki}}{I_{mn}} = \frac{A_{ki} g_k \lambda_{mn}}{A_{mn} g_m \lambda_{ki}} \exp\left(-\frac{E_k - E_m}{kT_e}\right). \quad (6)$$

Similarly, knowing the electron temperature and comparing the intensities of the lines of atoms (I) and single ions (II), we can estimate the number concentration of electrons [8, 17, 18]:

$$\frac{I^{II}_{ki}}{I^{I}_{mn}} = 2 \frac{A^{II}_{ki} g^{II}_k \lambda^{I}_{mn}}{A^{I}_{mn} g^{I}_m \lambda^{II}_{ki}} \left(\frac{2\pi m_e k T_e}{h^2}\right) \frac{1}{n_e} \times \exp\left(-\frac{E^{II}_k - E^{I}_m + E^{+}_k}{kT_e}\right). \quad (7)$$

To determine the electron temperature, atomic argon lines at 434.51, 750.38, and 811.38 nm with the highest radiation transition probability were selected [8, 10]. To improve the accuracy of the measurements, three lines were calculated and the result was averaged. To estimate the electron number density, a single argon ion line at 406.511 nm was selected. Relative intensities in this calculation were compared with the already used atomic lines at 434.51, 750.38, and 811.38 nm [16, 19].

The overall conversion of boron trichloride was determined by IR spectroscopy with an accuracy of 3 mol %. The measurements were carried out on a Bruker Vertex 80v spectrometer. The yield of boron condensed was determined gravimetrically with an accuracy of 1×10^{-3} g. The X-ray diffraction study of the obtained samples of boron powder was performed on an XRD-7000 diffractometer. The surface morphology of the boron powder was studied by scanning electron microscopy using a SUPRA 50VP and a NEON 40 electron microscopes (Carl Zeiss, Germany). The elemental composition of the samples was determined using the X-ray microanalysis method on an Oxford Instruments spectrometer. The impurity composition was determined by laser mass spectrometry using an EMAL-2 instrument. Raman spectra were measured on an NT-MDT NTEGRA Spectra instrument by using a laser with a wavelength of 473 nm. The radiation was focused using a 100× lens with an aperture of NA = 0.95. The particle size of the powder was determined on a Shimadzu SALD 2300 particle size analyzer by laser diffraction.

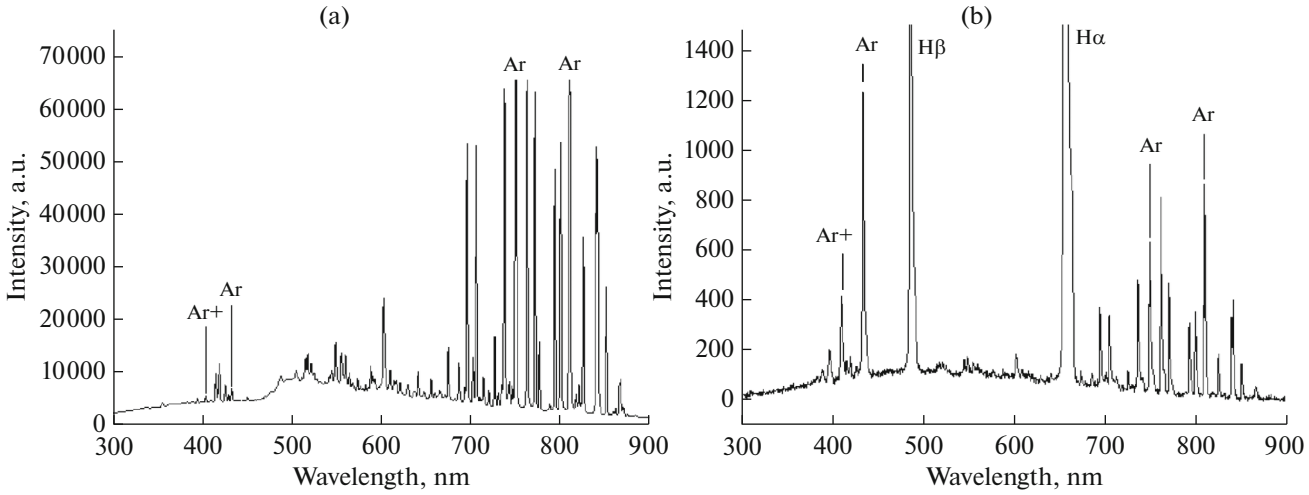

Fig. 2. Characteristic emission spectra of the RFI discharge: (a) Ar plasma; (b) Ar + H_2 plasma ($Ar/H_2 = 4$, $P = 1$ atm).

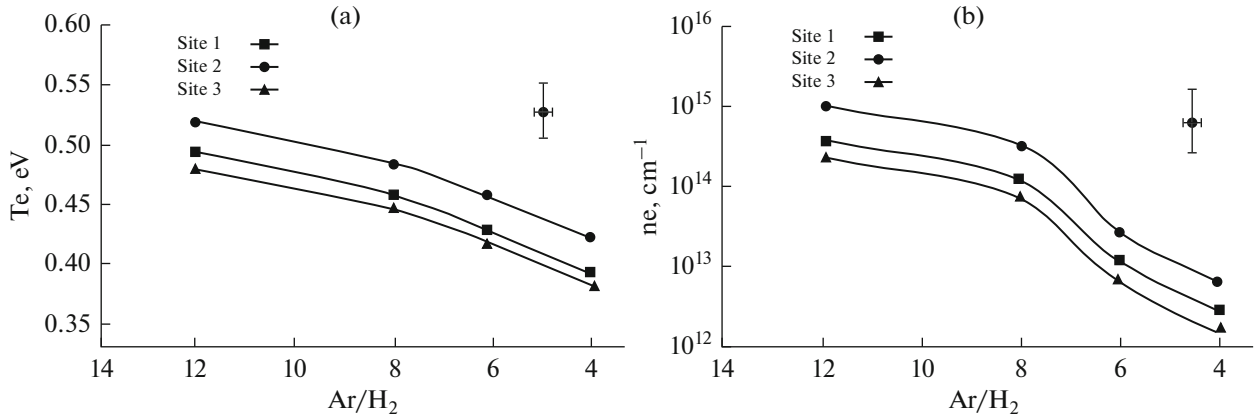

Fig. 3. Electron (a) temperature and (b) number density as functions of the Ar/H_2 ratio.

RESULTS AND DISCUSSION

Figure 2 shows the characteristic emission spectra of RFI argon and Ar + H_2 plasmas mixture at atmospheric pressure. The emission spectrum of the Ar + H_2 mixture exhibits bands at 486.13 and 656.2 nm assigned to atomic hydrogen H_β and H_α, respectively, and no Fulcher α-bands of molecular hydrogen in the region of 575–625 nm. These features indicate the almost complete dissociation of hydrogen under the given experimental conditions. Therefore, it can be assumed that the electron temperature T_e can be estimated for the Ar + H_2 mixture.

The electron temperature determined by the intensity ratio of the argon spectral bands and the number concentration of electrons in pure argon plasma (Fig. 2a) are 0.88 eV and 7.6×10^{14} cm^{-3}, respectively. When hydrogen is added, the electron temperature sharply decreases to 0.52 eV and further monotonically decreases with a decrease in the Ar/H_2 ratio (increase in the hydrogen concentration in the Ar + H_2 mixture) to be 0.42 eV at $Ar/H_2 = 12$. The electron number concentration decreases to 8×10^{12} cm^{-3} (Fig. 3b). The temperature and concentration of the electron gas obtained for the extreme points of the plasma torch are 10% less than those in the central part. It can be assumed that when hydrogen is added to the plasma-forming gas, a significant part of the energy is spent on its dissociation. This assumption is confirmed by the absence of Fulcher α-bands of molecular hydrogen in the emission spectra (Fig. 2b).

According to the estimations made for the gas temperature, the active species Ḣ possessing also reducing properties can be formed under these experimental conditions, as follows from [20]. The number concentration of atomic hydrogen at a temperature of 2500 K

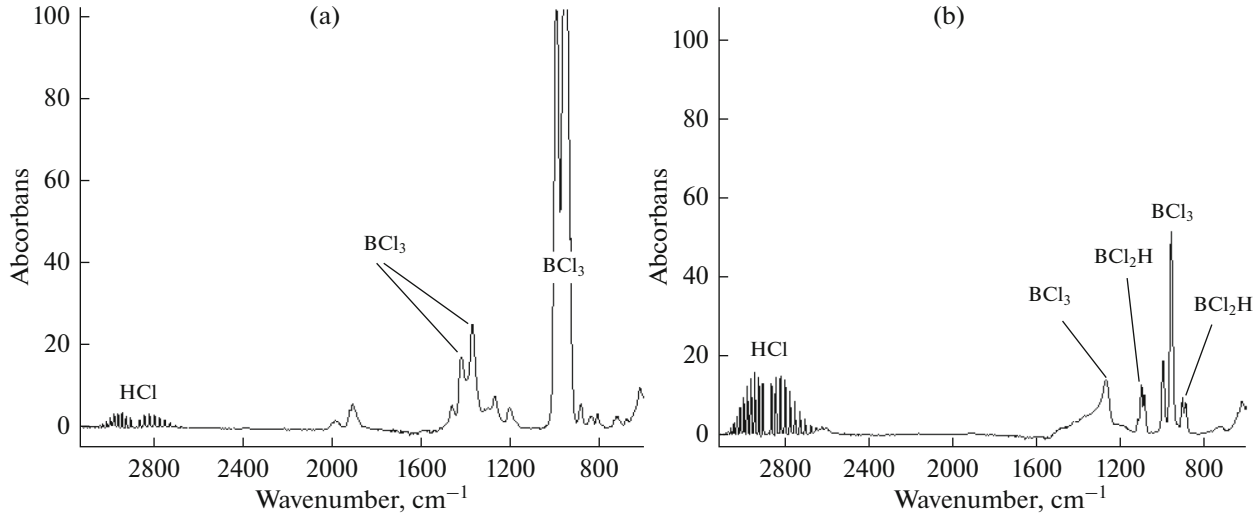

Fig. 4. IR spectrum of (a) the feed mixture of $BCl_3 + H_2 + Ar$ and (b) gaseous products at the outlet of the plasma reactor.

is as high as 6×10^{15} cm^{-3}. Hydrogen is atomized at $T_g \geq 2000$ K according to the reaction:

$$H_2 \rightarrow 2H. \quad (8)$$

In addition, argon atoms in the metastable state Ar* are present in the plasma; their lifetime is ≈ 1.3 s [20].

$$Ar + e \rightarrow Ar^* + e. \quad (9)$$

The formation of these species determines the pathway of particular plasma-chemical reactions in which they participate. Among them, we consider the hydrogen reduction of boron trichloride (BCl_3). In accordance with [21], the following species are produced in noticeable amounts from BCl_3 in plasma at the given gas temperatures: BCl_2 in the range of 2500–3000 K, BCl at 2500–4500 K, and Cl at 2500–5500 K. Nester et al. [22] made a kinetic analysis of the $BCl_3 + H_2$ system and noted that the hydrogen reduction of boron trichloride to B_{solid} proceeds through intermediate radicals BCl_2 and BCl to form volatile intermediate compounds $BHCl_2$ and BH_2Cl. In the case of introduction of the chemically active mixture $BCl_3 + H_2$ into the high-temperature zone and the possibility of formation of the active species Ar* and H$^\bullet$, the following intermediate reactions can be assumed:

$$BCl_3 + Ar^* \rightarrow BCl_2 + Cl + Ar, \quad (10)$$

$$BCl_2 + H \rightarrow BHCl_2, \quad (11)$$

$$BCl_2 + Ar^* \rightarrow BCl + Cl + Ar, \quad (12)$$

$$BCl + 2H \rightarrow BH_2Cl, \quad (13)$$

$$BCl + Ar^* \rightarrow B_{solid} + Cl + Ar, \quad (14)$$

$$H + Cl \rightarrow HCl. \quad (15)$$

Main Chemical Reactions in Boron Synthesis

Hydrogen reduction processes are always carried out under conditions of excess hydrogen concentration [23]. However, for the realized experimental conditions at a molar ratio of $Ar/H_2 = 4$, as already noted, gas-dynamic instabilities are observed and the gas discharge is extinguished. Therefore, to analyze the possible reactions of hydrogen reduction of these substances under the given experimental conditions, it is advisable to choose the molar ratio of $Ar/H_2 = 6$. The H_2/BCl_3 ratio in the reduction process was kept constant at 10. To determine the degree of conversion of boron trichloride, the composition of the reactant mixture fed to the plasma torch and that of the gaseous products were compared by using IR spectroscopy. The IR spectrum of the feed $BCl_3 + H_2 + Ar$ mixture is shown in Fig. 4a. From the spectrum of the feed mixture, it can be seen that it contains bands at 954, 993, 1372, 1421, and 1908 cm^{-1} due to boron trichloride (BCl_3). Insignificant amounts of dichloroborane (BCl_2H) and hydrogen chloride (HCl) are present as impurities, the bands of which are observed at 720, 886, and 3000 cm^{-1}, respectively. In the spectrum of the gaseous products (Fig. 4b), a significant decrease in the intensity of the bands assigned to BCl_3 is observed. In addition, there are bands with maxima at 900, 1083, and 1097 cm^{-1} due to dichloroborane. No bands due to monochloroborane are observed in the IR spectrum of the products. Therefore, it can be considered that reaction (13) does not proceed. The principal chemical reactions under the experimental conditions used are those to form boron and dichloroborane:

$$BCl_3 + 3H_2 \rightarrow 2B + 6HCl, \quad (16)$$

$$BCl_3 + H_2 \rightarrow BCl_2H + HCl. \quad (17)$$

Table 1. Concentration of impurities in boron sample

Element	*C*, at %	Element	*C*, at %
C	≈1.3	K	4×10^{-4}
N	≈0.8	Ca	4×10^{-3}
O	≈2.1	Ti	4×10^{-4}
F	3×10^{-3}	Cr	8×10^{-3}
Na	1×10^{-3}	Fe	5×10^{-2}
Mg	1×10^{-3}	Ni	4×10^{-3}
Al	3×10^{-2}	Mn	9×10^{-4}
Si	7×10^{-3}	Cu	1×10^{-4}
P	2×10^{-4}	Zn	3×10^{-4}
S	$\leq 3 \times 10^{-3}$	Ge	$<4 \times 10^{-5}$
Cl	1.5	W	$<1 \times 10^{-4}$

With an accuracy of 3%, the total conversion of boron trichloride is 75%, of which 10% is converted into the byproduct dichloroborane and 65% is to make the desired product boron.

The assessment of the degree of boron trichloride conversion to boron by the composition of the gas effluent from the reactor is confirmed by calculating the material balance taking into account the substrate (BCl_3) consumption and the collected solid phase boron.

Study of Morphology and Structure of Boron Samples

Figure 5 shows the morphology of B samples and the elemental composition according to X-ray fluorescence spectroscopy. The boron sample is made of fine particles, the size of which generally does not exceed 200 nm (Fig. 5a). The sample obtained using boron trichloride (Fig. 5b), in addition to the main component (boron, 98.1 wt %), contains oxygen and chlorine, the concentrations of which are 0.9 and 1.0 wt %, respectively.

The X-ray diffraction pattern of the sample is shown in Fig. 6. The main phase is identified as β-boron with a rhombohedral cell. The size of coherent-scattering regions estimated by peak width is 15 nm. The second phase identified on the X-ray diffraction pattern is that of boric acid. This explains the presence of oxygen in the sample.

Table 1 shows the impurity composition of a B sample. It is noteworthy that there are admixture of carbon, nitrogen, oxygen, and chlorine impurities. The increased oxygen content is apparently due to the presence of boric acid, which is also confirmed by the X-ray diffraction and X-ray fluorescence data. The

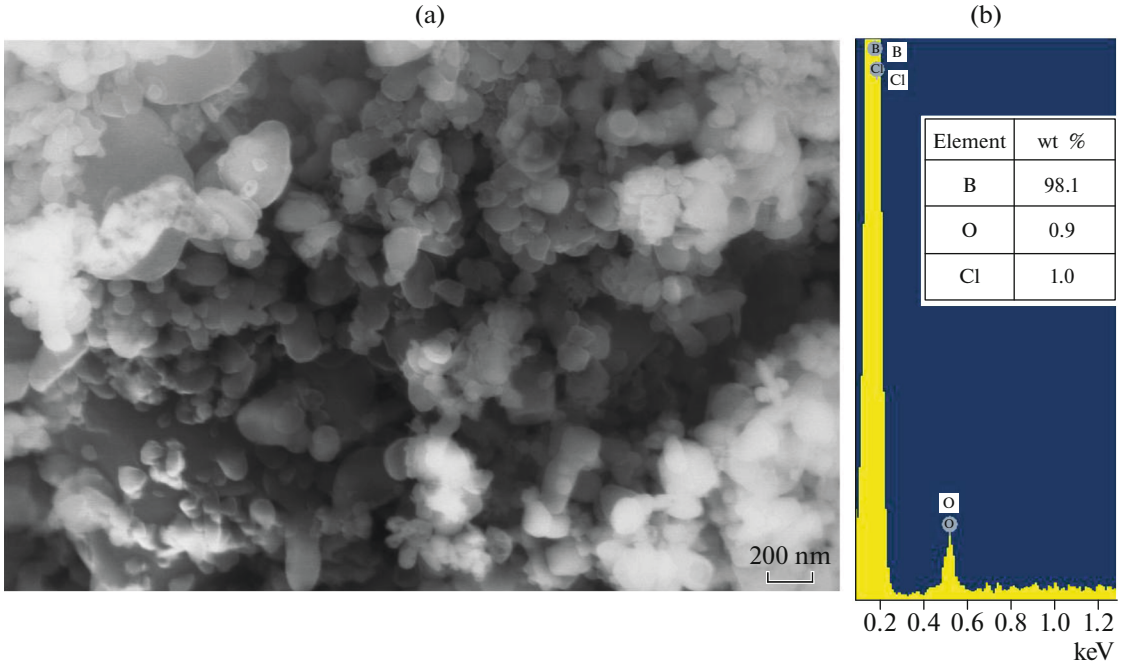

Fig. 5. (a) Morphology and (b) elemental composition of a boron sample obtained by boron trichloride reduction.

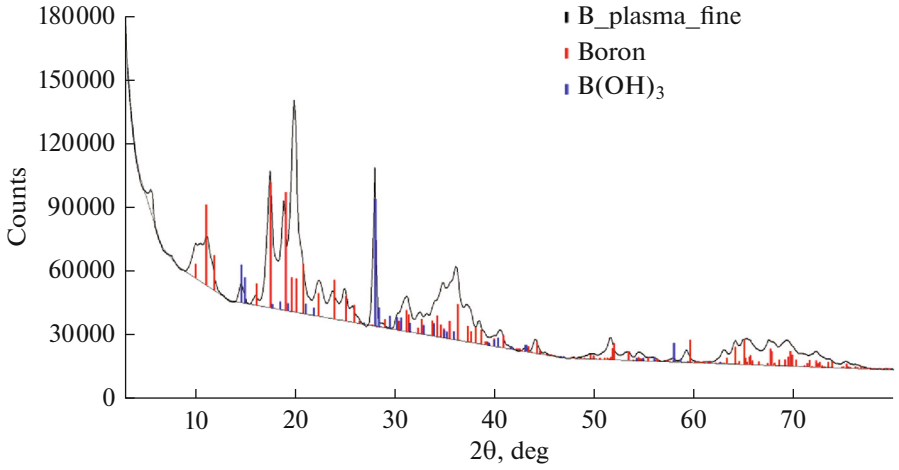

Fig. 6. Powder X-ray diffraction of finely divided boron.

carbon most likely comes from the filter materials. Chlorine is due to the reduction of boron trichloride and is also identified by the X-ray fluorescence analysis. The nitrogen impurity is present in the sample because of its absorption from air.

The Raman spectra (Fig. 7a) obtained from several points of the sample show several narrow and intense peaks at 440 and 761 cm^{-1} against the background of broad bands characteristic of amorphous systems. In addition, against the background of broad bands, narrow peaks of low intensity are observed at 350, 479, 536, 584, 620, 645, 670, 814, 864, and 940 cm^{-1}. As a feature, we can distinguish a band at 1100 cm^{-1} which is characteristic of crystalline β-boron [24]. The obtained data correlate with the powder X-ray diffraction data (Fig. 6).

Studying the particle size composition of the B powder sample (Fig. 7b), we obtained a distribution from 0.145 to 4.562 μm with a distribution maximum at 0.333 μm; the second less pronounced maximum was at 1.984 μm. In general, 99.9% of particles have a size not exceeding 3.755 μm, and 50% of the total volume of particles are smaller than 0.443 μm. The data obtained disagree with the data on the particle size obtained using a scanning electron microscope. This discrepancy can be explained by the agglomeration of particles with sizes of 200 nm or less. The resulting agglomerate cannot be divided using ultrasound in the course of sample preparation .

CONCLUSIONS

The studies performed allowed us to determine the optimum operating mode of a tangential-feed RFI plasma torch using an Ar + H_2 mixture as a plasma-forming gas. Under optimal conditions, the temperature and the number concentration of electrons in the

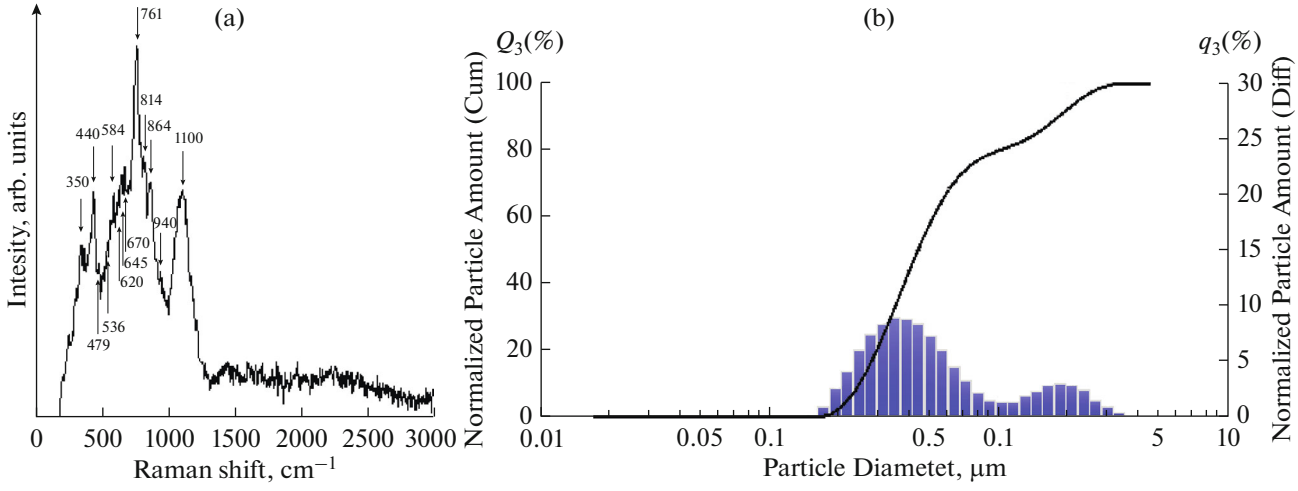

Fig. 7. (a) Raman spectrum of powdered boron and (b) its particle size composition.

inductor region were determined depending on the Ar/H_2 ratio. The calorimetric method was used to estimate the gas temperature. In addition, the process of hydrogen reduction of boron trichloride was studied under optimal conditions. It was shown that dichloroborane and polycrystalline boron are the main products. Boron nanopowder with a characteristic size of 200 nm was obtained. The amount of impurities in the resulting sample is 1×10^{-3} at %.

ACKNOWLEDGMENTS

This work was supported by the Russian Science Foundation, grant no. 17-13-01027). Authors thank the Ministry of Science and Higher Education of the Russian Federation (project no. 0095-2016-0006) for providing analytical equipment for characterization of the material.

REFERENCES

1. Reed, T.B., *J. Appl. Phys.*, 1961, vol. 32, p. 821.
2. Eckert, H.U., Report SAMSO-TR-227, Los Angeles: Space and Missile Systems Organization, 1972.
3. Mazin, V.I., RU Patent 2233563, 2004.
4. Frolov, V., Matveev, I., Ivanov, D., Zverev, S., Ushin, B., and Petrov, G., *Rom. J. Phys.,* 2011, vol. 56, p. 36.
5. Matveev, I., Matveyeva, S., and Zverev, S., *IEEE Trans. Plasma Sci.*, 2014, vol. 42, p. 3891.
6. Vetrov, S.I., Spitsyn, A.V., Shuvaev, D.A., and Yanchenkov, S.V., *Plasma Phys. Rep.*, 2006, vol. 32, p. 418.
7. Gol'dfarb, V.M. and Dresvin, S.V., *Teplofiz. Vys. Temp.*, 1995, vol. 3, p. 333.
8. Isola, L.M., Gómez, B.J., and Guerra, V., *J. Phys. D: Appl. Phys.*, 2010, vol. 43, p. 01520.
9. Greene, B.R., Clemens, N.T., Varghese, P.L., Bouslog, S.A., and Del Papa, S.V., *55th AIAA Aerospace Sciences Meeting, Grapevine, Texas, 9–13 January 2017*, AIAA SciTech Forum, (AIAA 2017-0394).
10. Laux, C.O., Spence, T.G., Kruger, C.H., and Zare, R.N., *Plasma Sources Sci. Technol.*, 2003, vol. 12, p. 125.
11. Diana, M., Russo, G., and Mario, L., *Proceedings of International Round Table on Study and Applications of Transport Phenomena in Thermal Plasmas*, Bonnet, C. Ed., Odeillo: CNRS, 1975, Rep. 1.8.
12. Cueilleron, J. and Cruiziat, B., *Bull. Soc. Chim. Fr.*, 1973, vol. 4, p. 1207.
13. Murdoch, H.D. and Hamblyn, S.M.L., US Patent 3625846, 1971.
14. Kelina, I.Yu., Ershova, N.I., Arakcheev, A.V., et al., *Refract. Ind. Ceram.*, 2004, vol. 45, p. P. 185.
15. Rusanov, V.D. and Fridman, A.A., *Physics of Chemically Active Plasma*, Boca Raton: CRC, 2007.
16. Han, G. and Cho, G., *Appl. Sci. Converg. Technol.*, 2017, vol. 26, p. 201.
17. Zhu, X.-M. and Pu, Y.-K., *Plasma Sources Sci. Technol.*, 2008, vol. 17, p. 024002.
18. Iordanova, E., de Vries, N., Guillemier, M., and Mvan der Mullen J.J., *J. Phys. D: Appl. Phys.*, 2008, vol. 41, p. 015208.
19. Bityurin, V.A., Grigorenko, A.V., Efimov, A.V., Klimov, A.I., Korshunov, O.V., Kutuzov, D.S., and Chinnov, V.F., *High Temp.*, 2014, vol. 52, p. P. 31.
20. Raizer, Y.P., *Gas Discharge Physics*, Berlin: Spriger, 1991.
21. Nester, S.A., Potapkin, B.V., Levitskii, A.A., Rusanov, V.D., Trusov, B.G., and Fridman, A.A., *Kinetiko-statisticheskoe modelirovanie khimicheskikh reaktsii v gazovom razryade* (Kinetic–Statistical Modeling of Chemical Reactions in Gas Discharge), Moscow: TsNII Atominform, 1988.
22. Fridman, A., *Plasma Chemistry*, New York: Cambridge Univ. Press, 2008.
23. Tsvetkov, Yu.V. and Panfilov, S.A., *Nizkotemperaturnaya plazma v protsessakh vosstanovleniya* (Low-Temperature Plasma in Reduction Processes), Moscow: Nauka, 1980.
24. Lannin, J.S., *Solid State Commun.*, 1978, vol. 25, p. 363.

Translated by V. Avdeeva